Effect of Substitution of Methyl Groups on the Luminescence Performance of Ir^{III} Complexes: Preparation, Structures, Electrochemistry, Photophysical Properties and Their Applications in Organic Light-Emitting Diodes (OLEDs)

Sungouk Jung,[a] Youngjin Kang,*[b] Hyung-Sun Kim,[a] Yun-Hi Kim,[a] Chang-Lyoul Lee,[c] Jang-Joo Kim,[c] Sung-Koo Lee,[d] and Soon-Ki Kwon*[a]

Keywords: Electrochemistry / Electrophosphorescence / Iridium / Luminescence / N ligands

A series of dimethyl-substituted tris(pyridylphenyl)iridium(III) derivatives [(*n*-MePy–*n*′-MePh)$_3$Ir] [*n* = 3, *n*′ = 4 (**1**); *n* = 4, *n*′ = 4 (**2**); *n* = 4, *n*′ = 5 (**3**); *n* = 5, *n*′ = 4 (**4**); *n* = 5, *n*′ = 5 (**5**)] have been synthesized and characterized to investigate the effect of the substitution of methyl groups on the solid-state structure and photo- and electroluminescence. The absorption, emission, cyclic voltammetry and electroluminescent performance of **1**–**5** have also been systematically evaluated. The structures of **2** and **4** have been determined by a single-crystal X-ray diffraction analysis. Under reflux (> 200 °C) in glycerol solution, *fac*-type complexes with a distorted octahedral geometry are predominantly formed as the major components in all cases. Electrochemical studies showed much smaller oxidation potentials relative to Ir(ppy)$_3$ (Hppy = 2-phenylpyridine). All complexes exhibit intense green photoluminescence (PL), which has been attributed to metal-to-ligand charge transfer (MLCT) triplet emission. The maximum emission wavelengths of thin films of **1**, **3**, **4** and **5** at room temperature are in the range 529–536 nm, while **2** displays a blue-shifted emission band (λ_{max} = 512 nm) with a higher PL quantum efficiency (Φ_{PL} = 0.52) than those of complexes **1** and **3**–**5**; this is attributed to a decrease of the intermolecular interactions. Multilayered organic light-emitting diodes (OLEDs) were fabricated by using three (**2**, **3** and **4**) of these Ir^{III} derivatives as dopant materials. The electroluminescence (EL) spectra of the devices, which have the maximum peaks at 509–522 nm, with shoulder peaks near 552 nm, are consistent with the PL spectra in solution at 298 K. The devices show operating voltages at 1 mA/cm^2 of 4.9, 5.6, 5.1, and 4.6 V for Ir(ppy)$_3$, **2**, **3**, and **4**, respectively. In particular, the device with **2** shows a higher external quantum efficiency (η_{ext} = 11% at 1 mA/cm^2) and brightness (4543 cd/m^2 at 20 mA/cm^2) than Ir(ppy)$_3$ (η_{ext} = 6.0% at 1 mA/cm^2; 3156 cd/m^2 at 20 mA/cm^2) and other Ir(dmppy)$_3$ derivatives, (dmppy = dimethyl-substituted ppy), under the same conditions. The methyl groups at the *meta* (Ph) and *para* (Py) positions to the Ir metal atom have a great influence on absorption, emission, redox potentials and electroluminescence.

Introduction

Luminescent transition metal complexes, such as those of groups 9 or 10, are currently of great interest due to their various applications in photochemistry, organic light-emitting diodes (OLEDs), and chemical sensors for small molecules.[1] Among these transition metal complexes, Ir^{III} complexes have been regarded as excellent phosphorescent materials because of their ability to achieve maximum internal quantum efficiency, nearly 100%, as well as high external quantum efficiency in OLEDs.[2] Based on previous reports, a promising phosphorescent metal complex in OLEDs should have a short lifetime in the excited state and high phosphorescent efficiency. Based on these considerations, a number of researchers have focused recently on the development of cyclometallated (C^N)Ir^{III} complexes.[2] In particlar, luminescent Ir(ppy)$_3$ (Hppy = 2-phenylpyridine) derivatives have been described where adjustment of the band gap between the HOMO and LUMO energy levels could be achieved by modification of the substituents on the ppy rings.[3] Accordingly, to control the energy of the Ir(ppy)$_3$ system from blue light emission to red, a judicious incorporation of electron donors/acceptors as substituents on the ppy frameworks is an essential prerequisite.[4,5] For example, introduction of electron-donating groups to the pyridine ring and electron-withdrawing groups to the phenyl ring can cause a decrease of the HOMO level and an increase of the LUMO level, respectively, inducing a larger

[a] School of Applied Chemical Engineering and Engineering Research Institute, Gyeongsang National University
Chinju 660-701, South Korea
Fax: (internat.) + 82-55-753-6311
E-mail: skwon@nongae.gsnu.ac.kr
[b] Division of Science Education, Kangwon National University
Chuncheon 200-701, South Korea
kangy@kangwon.ac.kr
[c] School of Materials Science and Engineering, Seoul National University
Seoul 151-744, South Korea
[d] LG Electronic Institute of Technology
16 Woomyeon-Dong, Seocho-Gu, Seoul 137-724, South Korea
Supporting information for this article is available on the WWW under http://www.eurjic.org or from the author.

band gap than that of $Ir(ppy)_3$. Although extensive research on the investigation of luminescent properties of Ir^{III} derivatives containing two *ortho*-chelating (C^N) ligands and a bidentate ancillary LX (e.g. monoanionic chelating ligands, acac = acetylacetonate, pic = picolinate, sal = salicyliminate), and their use and performance as triplet emitters in EL devices has been well documented over several years, the illustration of the effect of substituents, such as simple functional groups, and the dependence on their positions on the phenyl or pyridine rings in the ppy backbone, still remains virtually unexplored.[1e,5] During our ongoing investigation of phosphorescent $Ir(ppy)_3$ derivatives, we have observed that attached methyl groups as substituents on the ppy ligand have a remarkable influence on the electrochemical and photophysical properties.[6] Our interest in the development of highly efficient phosphors for application in OLEDs has prompted us to synthesize $Ir(ppy)_3$ derivatives and investigate their photophysical and electroluminescent characteristics. The methyl moiety was chosen for the following reasons: (i) The emissions of $Ir(ppy)_3$ derivatives come from phosphorescence with triplet character of both ligand-centered ($\pi-\pi^*$) and MLCT (metal-to-ligand charge transfer) transitions. This phosphorescence is strongly affected by the triplet energy of the *ortho*-chelating C∧N ligands. Therefore substituents, even methyl groups, on the ppy rings could play a key role in the alteration of the triplet energy. (ii) Although a methyl group is a weaker electron-donating group than other functional groups (e.g. OMe, NR_2 etc.), incorporating the methyl group as a substituent on the ppy rings has an influence on the HOMO and/or the LUMO level, as well as the ^{3}MLCT state of the complex. Herein we describe the results of our systematic investigation on the preparation, structural characterization, electrochemical behavior, photophysical properties and the fabrication of multiplayer phosphorescent light-emitting devices of a series of *fac*-[Ir^{III}(dmppy)$_3$] complexes [Hdmppy = *n*-methyl-2-(*n′*-methylphenyl)pyridine].

Results and Discussion

Syntheses and Structures

The methyl-substituted ppy ligands were synthesized by the Suzuki coupling[7] reaction of 2-bromo-*n*-methylpyridine with the corresponding *n′*-methylphenylboronic acid in the presence of K_2CO_3 and [$Pd(PPh_3)_4$] catalyst (Scheme 1).

These ligands were obtained in good yields (70−90%). Complexes **1**−**5** were synthesized by a slight modification of the previous synthetic methodology reported by Watt et al.[8b] The reaction of [$Ir(acac)_3$] with the corresponding methyl-substituted ppy ligands at high temperature (> 200 °C), gave **1**−**5** in moderate yields. Even though the ligands methylated at the 6- or 3′-position were synthesized successfully in moderate yields, the complexation of these ligands with the Ir^{III} starting material hardly occurs under the same reaction conditions. We attribute this mainly to steric factors.

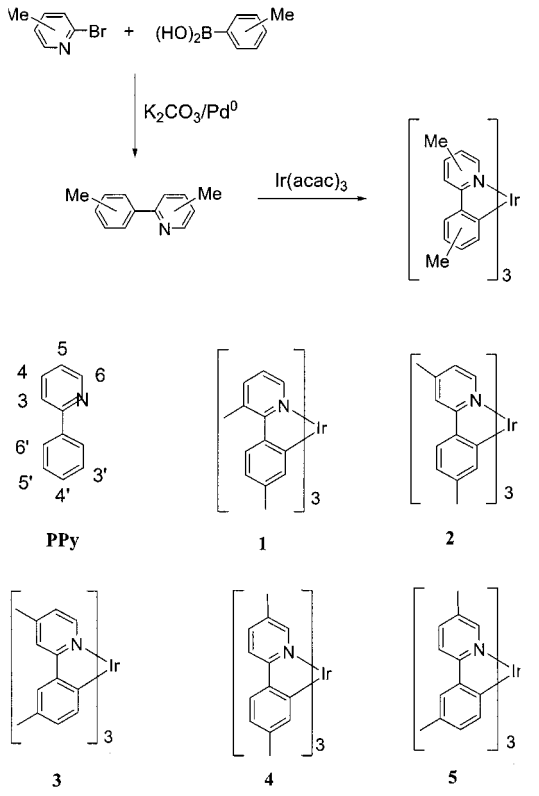

Scheme 1

There is a possibility of the formation of two isomers (*fac* and *mer*) during the reaction of $Ir(acac)_3$ and the Hdmppy ligands.[8a] However, we found that the *fac* isomer was formed as the major component, although some *mer* isomer was also formed. The formed *mer* isomers were not isolated because of their extremely low yields. All complexes are very stable up to 300 °C without degradation in air. In the ^{1}H NMR spectra, complexes **1**−**5** exhibit six well-resolved peaks due to the ppy rings, indicating that all complexes

Table 1. Selected bond lengths [Å] and angles [°] for **2** and **4**

Compound **2**			
Ir(1)−C(12)	2.015(8)	Ir(1)−C(38)	2.016(9)
Ir(1)−C(25)	2.034(8)	Ir(1)−N(1)	2.131(6)
Ir(1)−N(2)	2.114(7)	Ir(1)−N(3)	2.125(7)
C(12)−Ir(1)−N(1)	80.1(3)	C(38)−Ir(1)−N(3)	79.3(3)
C(25)−Ir(1)−N(2)	78.5(3)	C(12)−Ir(1)−C(38)	95.3(3)
C(38)−Ir(1)−N(1)	86.4(3)	C(38)−Ir(1)−C(25)	97.7(3)
C(38)−Ir(1)−N(2)	174.0(3)	C(12)−Ir(1)−C(25)	95.5(3)
Compound **4**[a]			
Ir(1)−C(12)	2.002(5)	Ir(1)−N(1)	2.111(5)
C(12)−Ir(1)−N(1)	79.3(2)	C(12A)^{i}−Ir(1)−C(12)	95.2(3)
C(12A)^{i}−Ir(1)−N(1B)^{ii}	171.6(2)	C(12)−Ir(1)−N(1B)^{ii}	91.6(2)
N(1B)^{ii}−Ir(1)−N(1)	94.48(19)		

[a] Symmetry transformations used to generate equivalent atoms: i: *z*, *x*, *y*; ii: *y*, *z*, *x*.

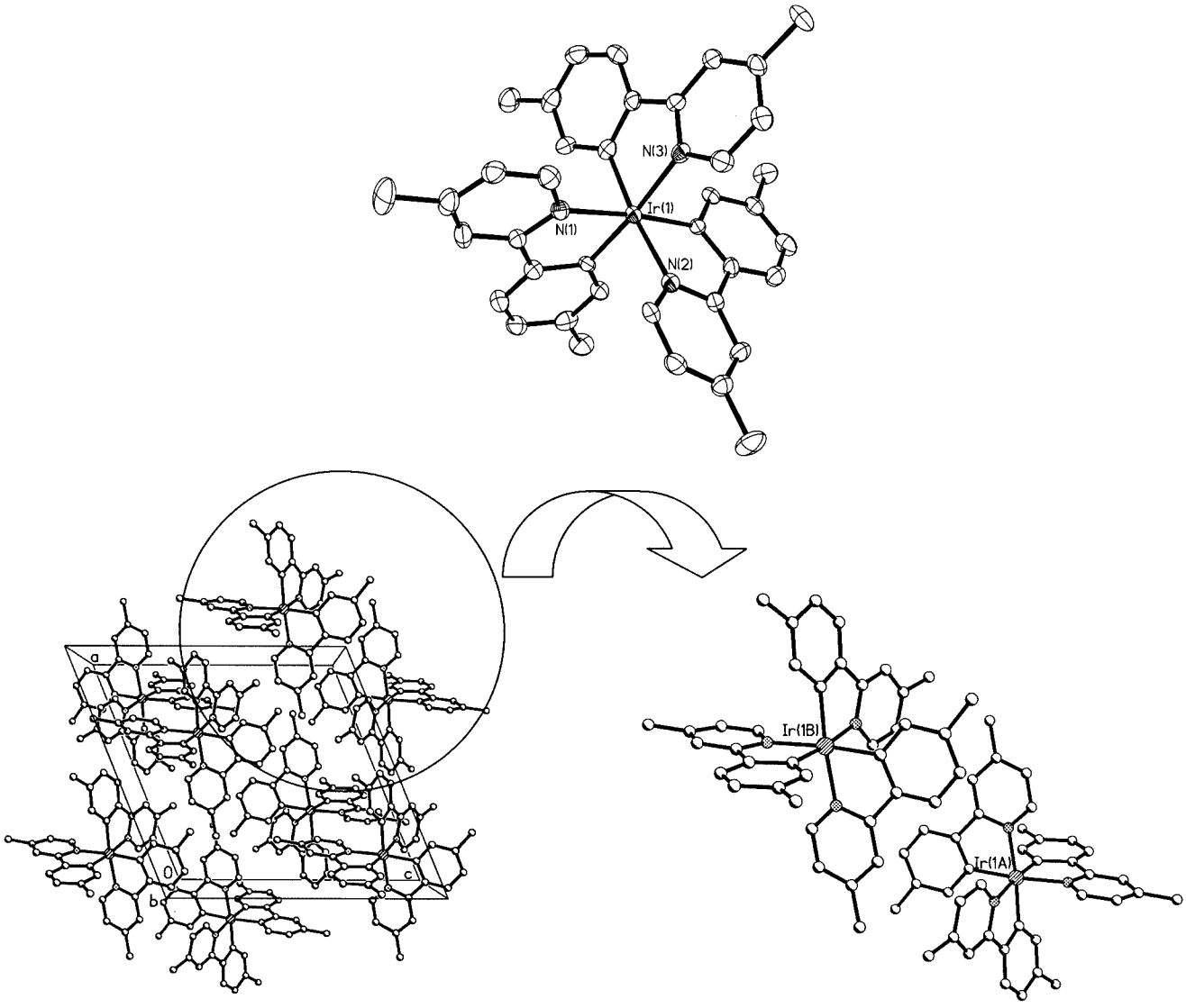

Figure 1. Top: Molecular structure of **2** with atom labeling schemes and 50% thermal ellipsoids; all hydrogen atoms have been omitted for clarity; bottom: crystal packing diagram between two adjacent molecules of **2** showing the lack of a π−π stacking interaction in the solid state

have a facial geometry around the Ir atom. Complexes **1**−**5** were fully characterized by mass spectrometry and elemental analyses, and crystal structures of **2** and **4** were obtained. Selected bond lengths and angles are presented in Table 1; refinement and structure-solution data can be found in the Exp. Sect. Complexes **2** and **4** exhibit only the *fac* configuration, with a distorted octahedral geometry around the Ir atom, as shown in Figures 1 and 2, respectively. The dihedral angle between the phenyl and pyridine rings in **2** (8.81°) is approximately three times larger than that of **4** (3.4°), indicating a decreased conjugation of the 4,4′-ppy ligands. The Ir−C bond lengths, ranging from 2.002(5) to 2.034 Å, are within the range reported for other mononuclear complexes with the $Ir(ppy)_2$ moiety [1.97(2)−2.13(6) Å],[9] and are also close to values reported for $[(tpy)_2Ir(\mu\text{-}Cl)_2Ir(tpy)_2]$ [Htpy = 2-(*p*-tolyl)pyridine] and other substituted *fac*-$[Ir(ppy)_3]$ derivatives.[8a,10] The σ-donor C atoms in the dmppy ligand arrange in a *trans* disposition to the dative N atoms of adjacent ppy ligands. The Ir−N bonds [2.111(5)−2.131 (6) Å] observed in **2** and **4** are slightly longer than those of $[Ir(acac)(tpy)_2]$ [2.040(5) Å] and $[Ir(acac)(ppy)_2]$ [2.010(9) Å].[5b] These observed elongations imply a stronger *trans* influence of the phenyl ring in comparison to the pyridyl groups having a *trans*-*N*,*N*′ configuration. In the crystal packing, **4** displays an effective overlap of the pyridine rings between two adjacent molecules (Figure 2). The shortest separation distance is about 3.22 Å, which is sufficiently short to suggest π−π stacking interactions. Complex **2** does not exhibit an effective overlap in the crystal packing, as shown in Figure 1. Recently, many reports have described that intermolecular π−π interactions have a direct influence on luminescent properties.[2c,5] The influence of this intermolecular interaction on the luminescence of the Ir^{III} complexes in this work is discussed below.

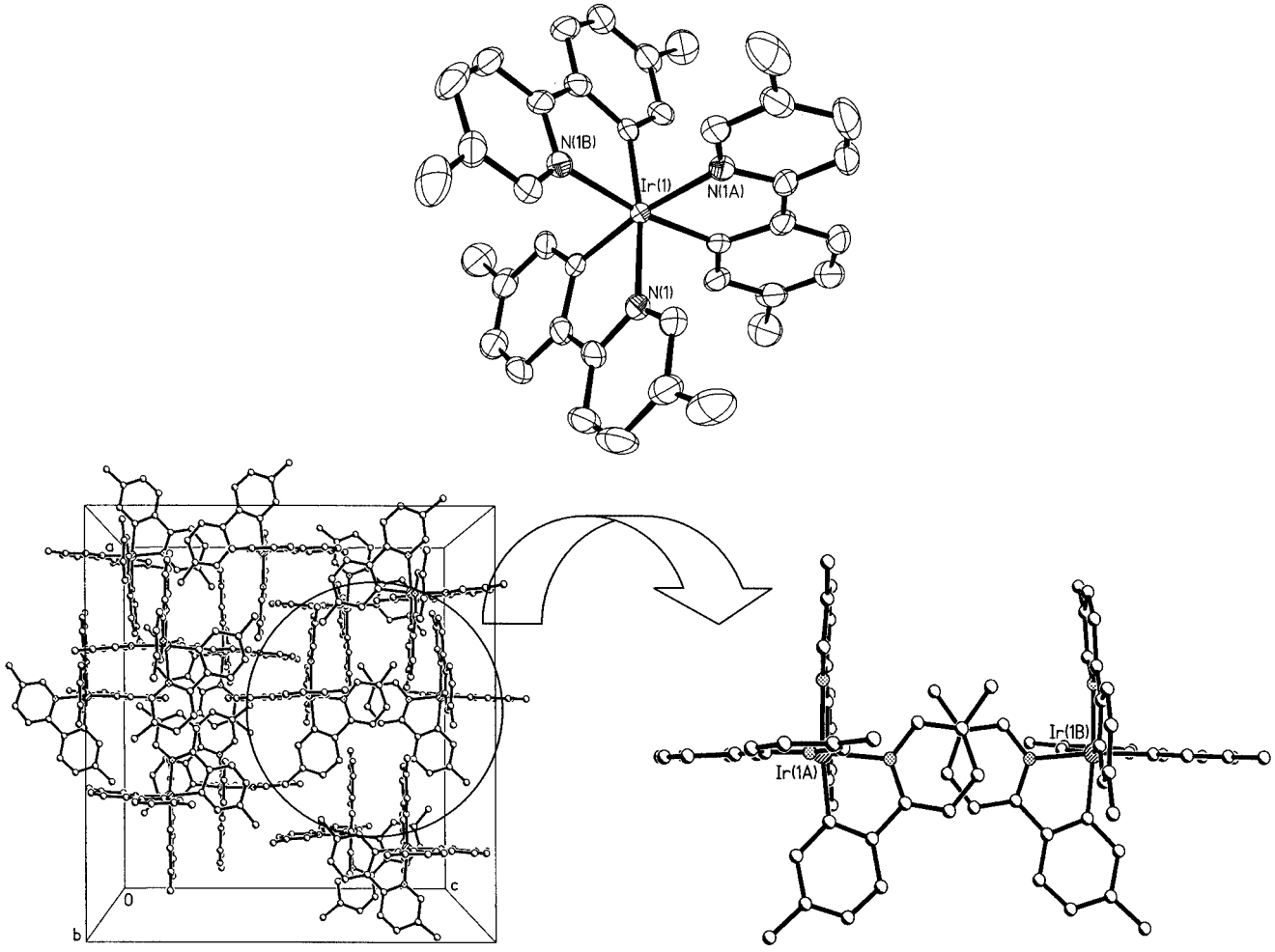

Figure 2. Top: Molecular structure of **4** with atom labeling schemes and 50% thermal ellipsoids; all hydrogen atoms have been omitted for clarity; bottom: crystal packing diagram between two adjacent molecules of **4** showing the intermolecular interaction in the solid state

Photoluminescent and Electrochemical Properties

Table 2 summarizes the photophysical data of **1**−**5**. The UV/Vis spectra of all compounds exhibit intense absorption bands between 250 and 310 nm ($\varepsilon > 10^4$ $mol^{-1}{\cdot}dm^3{\cdot}cm^{-1}$), indicating that the electronic transitions are mostly ligand-centered (LC) π−π * transitions (Figure 3). The absorption patterns of **1**−**5** and [Ir(ppy)$_3$] are similar in the 250−550 nm region.[11] However, the ^{1}MLCT and ^{3}MLCT peaks in **1**, **3**, **4** and **5** appear at lower energies than in [Ir(ppy)$_3$], while those of **2** occur at much higher energy with larger extinction coefficients. These observed blue- or red-shifted MLCT bands show that the methyl groups on the dmppy rings have a significant effect on the electronic

Table 2. Photophysical and electrochemical data of **1**−**5**[a] and [Ir(ppy)$_3$]

	UV (ε [10^3 $L{\cdot}mol^{-1}{\cdot}cm^{-1}$])	E_m (λ_{max}) Solution	Film	Φ_{PL}	Redox $E_{1/2}^{[ox]}$ [V]
[Ir(ppy)$_3$]	283(4.9), 380(4.1), 405(4.0), 455(3.5), 490(3.1)	514	516	0.40[b]	0.71
1	284(4.9), 384(4.1), 408(4.0), 455(3.6), 493(3.2)	522	529	0.41	0.51
2	278(4.9), 374(4.2), 407(4.0), 452(3.6), 484(3.3)	509	512	0.52	0.54
3	284(4.9), 391(4.1), 414(4.0), 456(3.6), 493(3.2)	524	534	0.32	0.49
4	284(4.9), 383(4.1), 412(4.0), 459(3.5), 493(3.2)	524	536	0.34	0.52
5	284(4.9), 384(4.0), 414(3.9), 458(3.4), 497(3.0)	524	532	0.29	0.47

[a] All the data were obtained in CH_2Cl_2 at ambient temperature with the same concentration. [b] Ref.[8a]

transition energies. The emission spectra of all complexes in solution and as thin films at room temperature are dominated by phosphorescence in the region 509−534 nm. Interestingly, both the absorption and emission spectra of **2** are blue-shifted relative to the other complexes and [Ir(ppy)$_3$]. This result can be explained by correlating the electronic and steric effects due to the methyl substituents. As reported previously,[5] the emission energy of [Ir(ppy)$_3$] can be controlled readily by adding substituents to the rings. To investigate the electronic effects caused by the addition of methyl groups, cyclic voltammetry experiments were carried out for all complexes, including [Ir(ppy)$_3$]. Due to the limited range available in CH_2Cl_2 and the inability of our instrument to measure the reduction potentials in the range −2.7 to −3.5 V, we obtained only the oxidation potentials for complexes **1**−**5** (Table 2). For the electrochemical behavior of Ir(ppy)$_3$ analogues it has been proposed that the oxidative and reductive processes involve the Ir−phenyl and −pyridine moiety of the C^N ligand, respectively. DFT calculations on a similar methyl-substituted Ir(ppy)$_3$ derivative, tris[2-(3-methylpyrid-2-yl)phenyl]iridium(III), provide evidence that the HOMO levels are mostly due to the Ir d_{z^2} orbital with some π-orbital contributions from the phenyl rings, while the LUMO levels in this complex are mostly due to the pyridine π* orbital.[8c] The same description complex has also been reported theoretically for the parent [Ir(ppy)$_3$] complex by Hay.[12] Reversible oxidation waves are observed for all complexes between 0.47 and 0.54 V. It is noteworthy that all of the complexes show lower oxidative potentials than [Ir(ppy)$_3$], indicating the relative ease of oxidation (see Figure 4). This can be ascribed to the great electron-donating ability of the methyl group. Complexes **3** and **5**, in particular, exhibit lower oxidation potentials than those of the other methyl-substituted complexes **1**, **2**, and **4**. Based on our DFT calculations, there are nodes at the 4′- and 6′-positions in the HOMO. In the HOMO, the electron density is mostly dispersed at the 3′- and 5′-positions, and also involves the 1′- and 2′-positions in the phenyl ring. Therefore, the donating effect from the methyl groups at either the 4′- or the 6′-position does not have a significant influence on the HOMO energy levels, while methyl groups at the 3′- or 5′-positions effectively donate electron density to the dmppy moiety, leading to a decrease in the oxidation potentials. The reduction process of the Ir(ppy)$_3$ derivatives was also shown to be due to the C^N ligand and is also affected by the various substituents.[8a] However, one of the key factors that affect the reduction potential in these systems is the degree of conjugation between the phenyl and pyridine rings. More effective conjugation stabilizes the LUMO, leading to a decreased reduction potential. Although we could not observe the reductive process, the reduction potential of **2** should be higher than that of complex **4**, as supported by the structural data.

Another fact affecting the nature of the luminescence in [Ir(ppy)$_3$] is the degree of steric hindrance. Lee et al. have demonstrated that higher photoluminescence quantum efficiencies (Φ_{PL}) and shorter lifetimes in [Ir(ppy)$_3$] derivatives can be achieved by the introduction of sterically hindered spacers, such as pinene.[2c] Although the effect on luminescence, such as excimer formation and from intermolecular π−π interactions, is less demonstrated in octahedral complexes than in square-planar Pt^{II} complexes,[13] these blue-shifted absorption and emission maxima for **2** could be attributed to a reduction of π-orbital conjugation between the phenyl and pyridine rings as well as the lack of intermolecular interactions in the solid state.[16] Therefore, we believe that the observed blue-shifted absorption and emission spectra of complex **2** are probably due to steric factors with a contribution from the strong electron-donating effect of the methyl group.

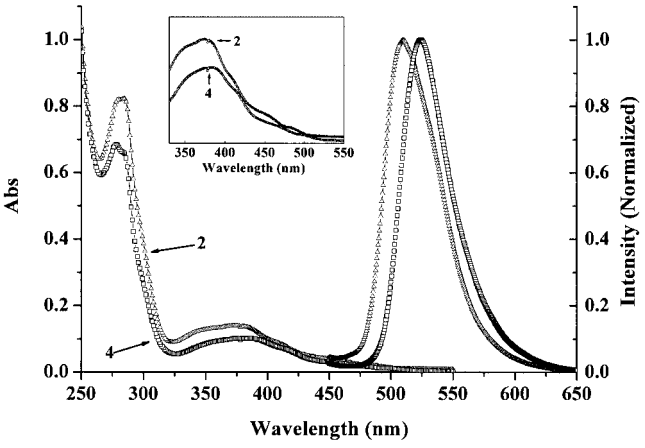

Figure 3. Absorption and emission spectra of **2** (triangles) and **4** (squares) in CH_2Cl_2 at room temperature; inset: MLCT bands of **2** and **4** in the UV/Vis region

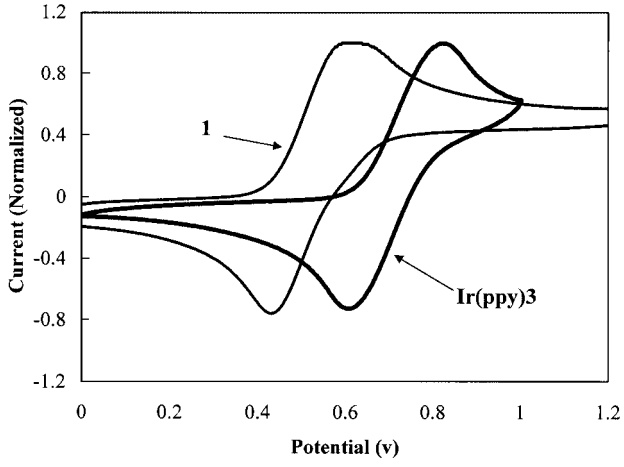

Figure 4. Cyclic voltammograms of **1** and [Ir(ppy)$_3$] in 0.1 M nBu$_4$NPF$_6$ at a scan rate of 50 mV/s

The PL quantum yields were obtained relative to [Ir(ppy)$_3$] (Φ_{PL} = 0.4) and increase in the order [Ir(4,4′dmppy)$_3$] (**2**) > [Ir(3,4′dmppy)$_3$] (**1**) > [Ir(5,4′dmppy)$_3$] (**4**) > [Ir(4,5′dmppy)$_3$] (**3**) > [Ir(5,5′dmppy)$_3$] (**5**). The observed high Φ_{PL} value for **2** can

be attributed partially to the reduction of intermolecular interactions. The lifetimes of the excited state in all complexes at room temperature are longer (> 1 μs) than that of [Ir(ppy)$_3$], indicating that the substituents generate a number of vibronic modes in the excited state of [Ir(dmppy)$_3$] (see Supporting Information).[15]

Based on our observation with respect to **2**, the blue-shifted emission energy, high PL efficiency and absence of intermolecular interactions are due to the incorporation of methyl groups at the *para* position of the pyridine and the *meta* position of the phenyl rings relative to the Ir atom. This phenomenon shows that the position of the substitution on the pyridine or phenyl rings as well as the electronic effect of the substituent have an influence on the phosphorescence of [Ir(ppy)$_3$] and related systems. When compared to the other positions, the 4- and 4′-positions are quite sensitive to both the photophysical and structural aspects.

Electroluminescent Properties

The electroluminescent properties of compounds **2**, **3** and **4** were investigated. Devices with the Ir phosphor doped into the emissive layer were fabricated. EL-device performance was conducted using complexes **2**, **3** or **4** as dopant and 4,4′-bis(9-carbazolyl)-1,1′-biphenyl (CBP) as host in all cases. In addition, to compare with previous works, EL devices with a similar structure were also fabricated with [Ir(ppy)$_3$], except for the cathode, as reported by Thompson et al.,[1b] by vacuum-deposition techniques. The device structure used in this work is a typical multi-layer, employing indium tin oxide (ITO) as the anode, copper-phthalocyanine (CuPc: 10 nm) as the hole injection material, 4,4′-bis[(1-naphthyl)(phenyl)amino]-1,1′-biphenyl (NPD: 40 nm) as the hole-transport material, **2**, **3**, or **4** as the dopant material, CBP as the host material (20 nm), 2,9-dimethyl-4,7-diphenyl-1,10-phenanthroline (BCP: 10 nm) as the hole-blocking material, aluminium tris(8-quinolinolate) (Alq$_3$: 40 nm) as the electron-transport material, LiF as the electron-injection layer, (1 nm) and Al (100 nm) as the cathode, as shown in Figure 5. All complexes display green emission in the range of 508−520 nm in the EL spectra, which are well matched to those of the PL spectra in solution. There are no characteristic emission peaks from CBP or Alq$_3$, indicating that the emission originates mostly from the dopant (Figure 6). Furthermore, these results support the proposal that effective energy transfer from the host (CBP) to the dopant (Ir complex) occurs in the emissive layer. More detailed EL characteristics are shown in Table 3. The turn-on voltages (defined as 1 mA/cm^2) of [Ir(ppy)$_3$], **2**, **3** and **4** are 3.4, 5.6, 5.1 and 4.6 V, respectively (Figure 7). The intermolecular interactions (e.g. π−π stacks in molecular crystals) in the solid state and the ability to trap charges in the emissive layer are considered the most important factors in determining the operating voltage. The strong electronic coupling and intermolecular interactions in the molecular crystals contribute to effective injection and transport of charges, leading to lower operating voltages.[16] On the other hand, effective charge-trapping by the dopants gives rise to increasing driving voltages in OLEDs.[17] If the dopant material functions as a hole trap, the HOMO level of the dopant could be above that of the host material. In other words, materials having a lower oxidation potential can function as effective hole traps in OLEDs. Therefore, the observed higher operating voltages for **2** and **4**, relative to [Ir(ppy)$_3$], are predominantly caused by effective hole trapping.[18] These results are consistent with the electrochemical behaviors of **1**−**5** and [Ir(ppy)$_3$]. The brightness of the devices at 20 mA/cm^2 are 4543 cd/m^2, 4470 cd/m^2, 3551 cd/m^2 and 3235 cd/m^2, for **2**, **3**, **4** and [Ir(ppy)$_3$], respectively. With increasing current density, the external quantum efficiency of devices containing **2**, **3**, **4** and [Ir(ppy)$_3$] gradually decreased. Similar results have been reported previously, and are attributed to the increase of triplet-triplet annihilation of the exciton at high voltage levels. As expected, the device fabricated using complex **2** exhibits higher brightness and external quantum efficiency, as well as stronger EL intensity, than those of the other complexes or [Ir(ppy)$_3$] (see Figures 8 and 9). In contrast, the device efficiencies of **1** and **4** are lower than that of [Ir(ppy)$_3$] under the same conditions. The positions of the substituents as well as the nature of the substituents on the ppy rings could be important factors in achieving high electroluminescent efficiency in substituted Ir(ppy)$_3$ systems.

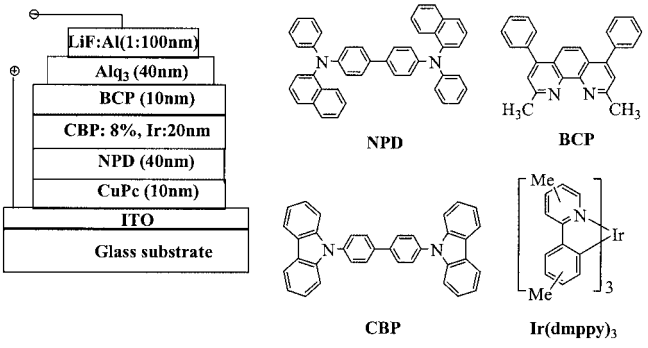

Figure 5. Device structures and molecular structure used in this study

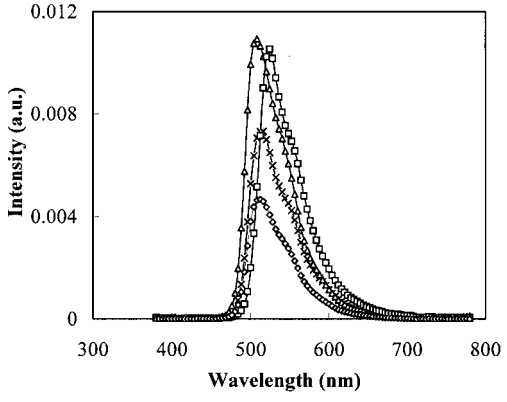

Figure 6. EL spectra of [Ir(ppy)$_3$], (X), **2** (triangles), **3** (squares) and **4** (diamonds) device structure: ITO/NPD/CBP-Ir(dmppy)$_3$/BCP/Alq$_3$/LiF-Al)

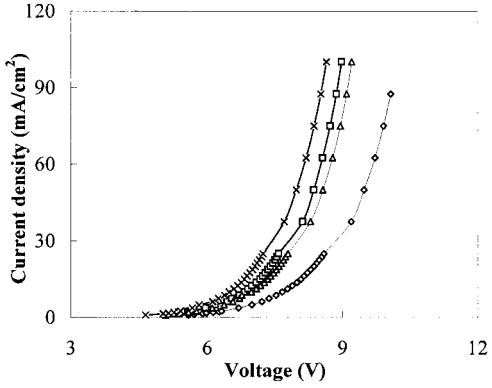

Figure 7. Voltage versus current-density characteristics of $[Ir(ppy)_3]$- (X), **2**- (triangles), **3**- (squares), and **4**-doped (diamonds) devices

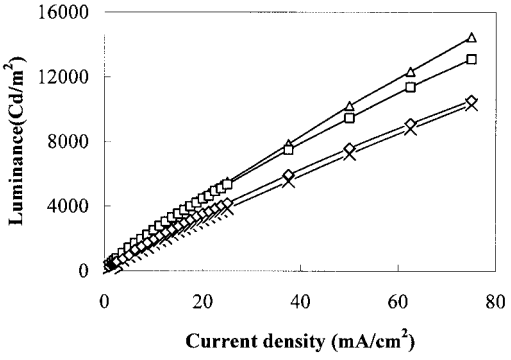

Figure 8. Luminance versus current-density characteristics of $[Ir(ppy)_3]$- (X), **2**- (triangles), **3**- (squares), and **4**-doped (diamonds) devices

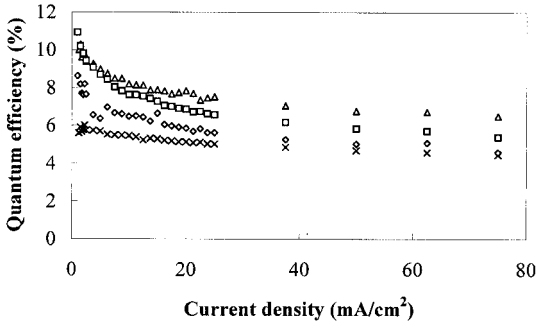

Figure 9. External quantum efficiency versus current-density characteristics of of $[Ir(ppy)_3]$- (X), **2**- (triangles), **3**- (squares), and **4**-doped (diamonds) devices

Conclusion

A series of dimethyl-substituted $[Ir(dmppy)_3]$ derivatives have been synthesized and characterized, including their photo-electroluminescent and electrochemical properties. The nature of their solid-state structures depends on the position of the methyl groups on the phenyl and pyridine rings. These methyl groups give rise to several distinct triplet states, affecting the electrochemical behavior and electroluminescence of the Ir^{III} complexes. As expected, they also considerably perturb the absorption, redox potentials, and photo- and electroluminescent efficiency. Lower oxidation potentials than that of $[Ir(ppy)_3]$ were observed in all cases, indicating that the methyl group induces a relatively easy oxidation and leads to effective hole trapping. Complex **2**, which has methyl groups at the 4′- and 4-positions exhibits a brighter green emission and higher Φ_{PL} than $[Ir(ppy)_3]$. In addition, a significant improvement of the external quantum efficiency (η_{ext} = 11%), which is nearly 200% higher than that of $[Ir(ppy)_3]$, is also observed in OLEDs. Further investigation on the effects on luminescent properties depending on other bulky functional groups into various positions of the ppy ligand is currently in progress.

Experimental Section

General Considerations. All experiments were performed under dry N_2 using standard Schlenk techniques. All solvents were freshly distilled from appropriate drying reagents prior to use. All starting materials were purchased from either Aldrich or Strem and used without further purification. Methyl-substituted phenyl or pyridine compounds were synthesized by slight modification of previous reports.[8]

Measurements: ^1H NMR and mass spectra were recorded with a Bruker DRX 500 MHz spectrometer and JEOL-JMS 700 instrument, respectively. UV/Vis and photoluminescent spectra for all samples with concentrations in the range of 10−50 μM were obtained with a Lambda 900 UV/Vis spectrometer and a Perkin−Elmer Luminescence spectrometer LS 50B. All solutions for photophysical experiments were degassed with more than three repeated freeze-pump-thaw cycles in a vacuum line. Melting points were determined with an Electrothermal 9100 apparatus. Emission lifetimes were measured with the fourth harmonic of a Q-switched Nd-YAG laser using the upper excited state energy transfer with a pulse duration of 6 ns and a repetition rate of 10 Hz. The laser beam had a diameter of 5 mm and an optical power of about 50 mJ. The emission from the film was recorded by a gated intensified diode array detector through a monochromator. The system allows for an integration time (gate width) of detection from 100 ns to 10

Table 3. Electroluminescent data of $[Ir(ppy)_3]$ and **2**-, **3**- and **4**-doped OLEDs

	Luminance [Cd/m²] at 20 mA/cm²	Operating voltage [V][a]	External quantum efficiency (%) at 1 mA/cm²	at 10 mA/cm²	at 50 mA/cm²
$Ir(ppy)_3$	3156	4.9	6.0	5.4	4.7
2	4543	5.6	11	8.2	6.8
3	4470	5.1	10.9	7.6	5.8
4	3551	4.6	8.6	6.5	5.0

[a] The operating voltages in all cases were defined as 1 mA/cm².

ms and a variable delay after excitation. Cyclic voltammetry was performed with an Autolab potentiostat from Echochemie under nitrogen in a one-compartment electrolysis cell consisting of a platinum wire working electrode, a platinum wire counter electrode, and a quasi Ag/AgCl reference electrode. Cyclic voltammograms were monitored at scan rates of either 100 $mV \cdot s^{-1}$ or 50 $mV \cdot s^{-1}$ and recorded in distilled dichloromethane. The concentration of the complex was maintained at 0.5 mM or less and each solution contained 0.1 M of tetrabutylammonium hexafluorophosphate (TBAP) as the electrolyte. The ferrocenium/ferrocene couple (0.40V) was used as the internal standard.

X-ray Crystallographic Analysis: Suitable crystals of **2** and **4** were obtained from slow vapor diffusion of toluene/benzene/hexane (2:1:1) into a solution of **2** or **4** in CH_2Cl_2. The crystal of **2** or **4** was attached to a glass fiber and mounted on a Bruker SMART diffractometer equipped with a graphite-monochromated Mo-K_α (λ = 0.71073 Å) radiation, operating at 50 kV and 30 mA and a CCD detector; 45 frames of two-dimensional diffraction images were collected and processed to obtain the cell parameters and orientation matrix. All data collections were performed at 173 K. The data collection 2θ ranges were 3.1−56.62° for **2** and 4.26−56.56° for **4**. No significant decay was observed during the data collection. The raw data were processed to give structure factors using the SAINT program. Each structure was solved by direction methods and refined by full-matrix least squares against F^2 for all data using the SHELXTL software (version 5.10).[19] All non-hydrogen atoms in compounds **2** and **4** were anisotropically refined. All other hydrogen atoms were included in the calculated positions and their contributions in structural factor calculations were included. Compound **2** cocrystallizes with benzene in the monoclinic crystal system with space group $P2_1/n$. The disordered benzene molecule was not modeled successfully. However, hydrogen atoms in benzene were included in the calculated positions and their contributions included in the structure factor. Compound **4** belongs to the cubic crystal system ($I\bar{4}3d$ space group). Crystal data for **2** and **4** are summarized in Table 4. Selected bond lengths and angles for **2** and **4** are given in Table 1. In the case of **2**, since the large positive (3.236 $e/Å^{-3}$) and negative (−3.306 $e/Å^{-3}$) difference Fourier peaks are located at short distances from Ir (0.84 Å and 0.90 Å, respectively), these peaks can be attributed to ghosts of the heavy Ir atom.[20] CCDC-220262 (**2**) and -220263 (**4**) contain the supplementary crystallographic data for this paper. These data can be obtained free of charge at www.ccdc.cam.ac.uk/conts/retrieving.html [or from the Cambridge Crystallographic Data Centre, 12 Union Road, Cambridge CB2 1EZ, UK; Fax: (internat.) + 44-1223-336 033; E-mail: deposit@ccdc.cam.ac.uk].

Fabrication of Electroluminescent Devices: A glass substrate precoated with indium tin oxide (ITO) was cleaned in an ultrasonic bath of acetone, followed by 2-propanol. Surface treatment was carried out by exposing ITO to a UV ozone plasma. OLEDs withg CBP as host material were fabricated as follows. The hole-injecting layer, a 10 nm thick film of CuPc was deposited on the ITO surface by high-vacuum thermal evaporation and a 40 nm thickness α-NPD as hole-transporting layer was deposited onto the CuPc. An [Ir(dmppy)$_3$]-doped (dmppy = dimethyl-substituted ppy) host CBP layer was thermally co-evaporated onto the α-NPD layer. The [Ir(dmppy)$_3$] doping concentration was 8% in CBP. A 10 nm thick BCP (2,9-dimethyl-4,7-diphenyl-1,10-phenanthroline) layer was then deposited as the exciton-blocking layer, followed by a 40 nm thick Alq_3 layer as an electron-transporting layer. Finally, LiF (1 nm) and Al (100 nm) were deposited on top of the organic layers by thermal evaporation. The fabricated multilayer organic light-emitting devices have the structure of ITO/CuPc (10 nm)/α-NPD (40 nm)/CBP-Ir(dmppy)$_3$ (20 nm)/BCP (10 nm)/Alq_3 (40 nm)/LiF (1 nm)/Al (100 nm).

Table 4. Crystallographic data for **2** and **4**

	2	**4**
Empirical formula	$C_{39}H_{36}IrN_3 \cdot 0.5C_6H_6$	$C_{39}H_{36}IrN_3$
Formula mass	777.96	738.91
Space group	$P2_1/n$	$I\bar{4}3d$
a [Å]	15.5695(9)	23.4008(10)
b [Å]	14.6261(8)	23.4008(10)
c [Å]	16.1088(9)	23.4008(10)
β [°]	111.8840(10)	90
V [Å^3]	3403.0(3)	12814.2(9)
Z	4	16
$D_{calcd.}$ [$Mg \cdot cm^{-3}$]	1.518	1.532
μ [cm^{-1}]	39.56	41.99
$2\theta_{max}$ [°]	56.62	56.64
No. of refections measured	21580	39294
No. of refections used	7996	2650
R_{int}	0.1391	0.1027
No. of parameters	415	130
Final R [$I > 2\sigma(I)$]		
$R1$[a]	0.0525	0.0341
$wR2$[b]	0.1182	0.0755
R (all data)		
$R1$[a]	0.0950	0.0429
$wR2$[b]	0.1582	0.0800
Goodness of fit on F^2	1.006	1.253

General Preparation of [Ir(n,n'-dmppy)$_3$]: The corresponding complexes were synthesized by a slight modification of Watt's procedures.[8b] A solution of the corresponding methyl-substituted phenylpyridine ligand (6 equiv., 2.64 mmol) in glycerol was added at ambient temperature under N_2 to a stirred anhydrous degassed glycerol solution (20 mL) of [Ir(acac)$_3$] (0.217 g, 0.44 mmol). The reaction mixture was refluxed for 24−48 h. The reaction mixture was then cooled to room temperature, 1 N HCl was added, and the mixture filtered to give a crude product. The pure complexes were obtained by chromatographic workup on silica gel using ethyl acetate/hexane as eluent.

[Ir(3,4′dmppy)$_3$] (1): ^{1}H NMR (CD_2Cl_2, 25 °C): δ = 7.86 (d, J = 8.4 Hz, 3 H), 7.46 (dd, J = 7.5, 0.9 Hz, 3 H), 7.36 (dd, J = 5.4, 1.5 Hz, 3 H), 6.67−6.78 (m, overlap, 9 H), 2.82 (s, 9 H, CH_3), 2.12 (s, 9 H, CH_3) ppm. MS (EI): m/z = 739 [M^+]. $C_{39}H_{36}IrN_3$ (739.25): calcd. C 63.39, H 4.91, N 5.69; found C 63.31, H 4.89, N 5.67.

[Ir(4,4′dmppy)$_3$] (2): ^{1}H NMR (CD_2Cl_2, 25 °C): δ = 7.71 (s, 3 H), 7.56 (d, J = 8.1 Hz,, 3 H), 7.36 (d, J = 5.47 Hz, 3 H), 6.71−6.74 (m, overlap, 6 H), 6.61 (dd, J = 1.2, 0.3 Hz, 3 H), 2.44 (s, 9 H, CH_3), 2.12 (s, 9 H, CH_3) ppm. MS (EI): m/z = 739 [M^+]. $C_{39}H_{36}IrN_3$ (739.25): calcd. C 63.39, H 4.91, N 5.69; found C 63.38, H 4.95, N 5.71.

[Ir(4,5′dmppy)$_3$] (3): ^{1}H NMR (CD_2Cl_2, 25 °C): δ = 7.74 (s, 3 H), 7.50 (s, 3 H), 7.42 (d, J = 5.7 Hz, 3 H), 6.75 (dd, J = 1.5, 0.9 Hz, 3 H), 6.64 (d, J = 0.6 Hz, 6 H), 2.44 (s, 9 H, CH_3), 2.27 (s, 9 H, CH_3) ppm. MS (EI): m/z = 739 [M^+]. $C_{39}H_{36}IrN_3$ (739.25): calcd. C 63.39, H 4.91, N 5.69; found C 63.40, H 4.86, N 5.61.

[Ir(5,4′dmppy)$_3$] (4): ^{1}H NMR (CD_2Cl_2, 25 °C): δ = 7.80 (d, J = 8.4 Hz, 3 H), 7.55 (d, J = 7.8 Hz, 3 H), 7.47 (ddd, J = 7.8, 2.1, 0.6 Hz, 3 H), 7.31 (dd, J = 1.2, 0.9 Hz, 3 H), 6.72 (dd, J = 7.8, 1.2 Hz, 6 H), 6.58 (d, J = 0.9 Hz, 3 H), 2.15 (s, 9 H, CH_3), 2.12 (s, 9 H, CH_3) ppm. MS (EI): m/z = 739 [M^+]. $C_{39}H_{36}IrN_3$ (739.25): calcd. C 63.39, H 4.91, N 5.69; found C 63.30, H 4.84, N 5.62.

[Ir(5,5′dmppy)$_3$] (5): ^{1}H NMR (CD_2Cl_2, 25 °C): δ = 7.83 (d, J = 8.4 Hz, 3 H), 7.50 (m, overlap, 6 H), 7.37 (dd, J = 1.2, 0.6 Hz, 3 H), 6.59−6.67 (m, overlap, 6 H), 2.27 (s, 9 H, CH_3), 2.17 (s, 9 H, CH_3) ppm. MS (EI): m/z = 739 [M^+]. $C_{39}H_{36}IrN_3$ (739.25): calcd. C 63.39, H 4.91, N 5.69; found C 63.43, H 4.85, N 5.67.

Supporting Information: Spectroscopic data (^{1}H NMR, mass, and absorption/emission spectra), lifetime determination, electrochemical data and crystal-packing diagrams.

Acknowledgments

This work was supported by LG Electronics' national program funded by the Ministry of Commerce, Industry and Energy (project code: 00014756), the Information Technology Research Center (ITRC) under the Ministry of Information & Communications and the Korea Research Foundation Grant (KRF-2002-050-C00010).

[1] [1a] M. A. Baldo, M. E. Thompson, S. R. Forrest, *Nature* **2000**, *403*, 750. [1b] M. A. Baldo, S. Lamansky, P. E. Burrows, M. E. Thompson, S. R. Forrest, *Appl. Phys. Lett.* **1999**, *75*, 4. [1c] C. Adachi, M. A. Baldo, S. R. Forrest, M. E. Thompson, *Appl. Phys. Lett.* **2000**, *77*, 904. [1d] R. Gao, D. G. Ho, H. Hernandez, M. Selke, D. Murphy, P. I. Djurovich, M. E. Thompson, *J. Am. Chem. Soc.* **2002**, *124*, 14828. [1e] S. Lamansky, P. I. Djurovich, D. Murphy, F. Abdel-Razzaq, H.-E. Lee, C. Adachi, P. E. Burrows, S. R. Forrest, M. E. Thompson, *J. Am. Chem. Soc.* **2001**, *123*, 4304. [1f] S. Lamansky, R. C. Kwong, M. Nugent, P. I. Djurovich, M. E. Thompson, *Org. Electrochem.* **2001**, *2*, 53. [1g] M. Ikai, S. Tokito, Y. Sakamoto, T. Suzuki, Y. Taga, *Appl. Phys. Lett.* **2001**, *79*, 156. [1h] C. Adachi, M. A. Baldo, S. R. Forrest, M. E. Thompson, *J. Appl. Phys.* **2001**, *90*, 5048. [1i] M-J. Yang, T. Tsutsui, *Jpn. J. Appl. Phys.* **2000**, *39*, L828. [1j] E. Vander Donckt, B. Camerman, F. Hendrick, R. Herne, R. Vandeloise, *Bull. Soc. Chim. Belg.* **1994**, *103*, 207. [1k] Y. Amao, Y. Ishikawa, I. Okura, *Anal. Chim. Acta* **2001**, *445*, 177. [1l] D. Song, S. Wang, *Eur. J. Inorg. Chem.* **2003**, *20*, 3744.

[2] [2a] D. F. O'Brien, M. A. Baldo, M. E. Thompson, S. R. Forrest, *Appl. Phys. Lett.* **1999**, *74*, 442. [2b] J.-P. Duan, P.-P. Sun, C.-H. Cheng, *Adv. Mater.* **2003**, *15*, 224. [2c] H. Z. Xie, M. W. Liu, O. Y. Wang, X. H. Zhang, C. S. Lee, L. S. Hung, S. T. Lee, P. F. Teng, H. L. Kwong, H. Zheng, C. M. Che, *Adv. Mater.* **2001**, *13*, 1245. [2d] Y.-Y. Noh, C.-L. Lee, J.-J. Kim, K. Yase, *J. Chem. Phys.* **2003**, *118*, 2853. [2e] Y. Wang, N. Herron, V. V. Grushin, D. LeCloux, V. Petrov, *Appl. Phys. Lett.* **2001**, *79*, 449. [2f] F. Neve, A. Crispini, S. Serroni, F. Loiseau, S. Campagna, *Inorg. Chem.* **2001**, *40*, 1093. [2g] G. Calogero, G. Giuffrida, S. Serroni, V. Ricevuto, S. Campagna, *Inorg. Chem.* **1995**, *34*, 541. [2h] F. Neve, A. Crispini, S. Campagna, S. Serroni, *Inorg. Chem.* **1999**, *38*, 2250. [2i] S. M. Zakeeruddin, M. K. Nazeeruddin, P. Pechy, F. P. Rotzinger, R. Humphry-Baker, K. Kalyanasundaram, M. Grätzel, V. Shklover, T. Haibach, *Inorg. Chem.* **1997**, *36*, 5937.

[3] [3a] C. Adachi, R. C. Kwong, P. Djurovich, V. Adamovich, M. A. Baldo, M. E. Thompson, S. R. Forrest, *Appl. Phys. Lett.* **2001**, *79*, 2082. [3b] Y. Kawamuura, S. Yanagida, S. R. Forrest, *J. Appl. Phys.* **2002**, *92*, 87. [3c] F.-C. Chen, Y. Yang, M. E. Thompson, J. Kido, *Appl. Phys. Lett.* **2002**, *80*, 2308.

[4] [4a] B. D. Alleyne, V. adamovich, J. Brooks, P. I. Djurovich, M. E. Thompson, *224th ACS National Meeting, USA* **2002**, INOR-204. [4b] M. E. Thompson, *4th ICEL (International Conference on Electroluminescence of Molecular Materials and Related Phenomena), Korea* **2003**, O-41.

[5] [5a] V. V. Grushin, N. Herron, D. D. LeCloux, W. J. Marshall, V. A. Petrov, Y. Wang, *Chem. Commun.* **2001**, 1494. [5b] S. Lamansky, P. Djurovich, D. Murphy, F. Abdel-Razzaq, R. Kwong, I. Tsyba, M. Bortz, B. Mui, R. Bau, M. E. Thompson, *Inorg. Chem.* **2001**, *40*, 1704.

[6] [6a] S. O. Jung, Q. H. Zhao, H.-S. Kim, Y.-H. Kim, J.-S. Kim, C.-L. Lee, J.-J. Kim, B.-K. An, S. Y. Park, S.-K. Kwon, *224th ACS National Meeting, Boston, USA* **2002**, 18−22. [6b] S. O. Jung, Y.-H. Kim, Y.-H. Kim, Y. Kang, H.-Y. Oh, S.-K. Kwon, *226th ACS National Meeting, New York, USA* **2003**, 7−11. [6c]S. O. Jung, Y. Kang, H.-S. Kim, Y.-H. Kim, K. Yang, S.-K. Kwon, *Bull. Korean Chem. Soc.* **2003**, *24*, 1521. [6d] C.-L. Lee, K. B. Lee, J.-J. Kim, *Appl. Phys. Lett.* **2000**, *77*, 2280. [6e] R. R. Das, C.-L. Lee, Y.-Y. Noh, J.-J. Kim, *Opt. Mater.* **2002**, *21*, 143.

[7] Recent review: [7a] J. Hassan, M. Sévignon, C. Gozzi, E. Schulz, M. Lemaire, *Chem. Rev.* **2002**, *102*, 1359. [7b] A. Suzuki, *J. Organomet. Chem.* **1999**, *576*, 147.

[8] [8a] For a recent report, see: A. B. Tamayo, B. D. Alleyne, P. I. Djurovich, S. Lamansky, I. Tsyba, N. N. Ho, R. Bau, M. E. Thompson, *J. Am. Chem. Soc.* **2003**, *125*, 7377. [8b] K. Dedeian, P. I. Djurovich, F. O. Garces, G. Carlson, R. J. Watts, *Inorg. Chem.* **1991**, *30*, 1685. [8c] M. G. Colombo, T. C. Brunold, T. Riedener, H. U. Guedel, M. Fortsch, H.-B. Buergi, *Inorg. Chem.* **1994**, *33*, 545.

[9] [9a] R. Urban, R. Krämer, S. Mihan, K. Polborn, B. Wagner, W. Beck, *J. Organomet. Chem.* **1996**, *517*, 191. [9b] F. Neve, A. Crispini, *Eur. J. Inorg. Chem.* **2000**, 1039.

[10] F. O. Garces, K. Dedeian, N. L. Keder, R. J. Watts, *Acta Crystallogr., Sect. C* **1993**, *49*, 1117.

[11] [11a] K. Ichimura, T. Kobayashi, K. A. King, R. J. Watts, *J. Phys. Chem.* **1987**, *91*, 6104. [11b] K. A. King, P. J. Spellane, R. J. Watts, *J. Am. Chem. Soc.* **1985**, *107*, 1431.

[12] P. J. Hay, *J. Phys. Chem. A* **2002**, *106*, 1634.

[13] [13a] S.-C. Chan, M. C. W. Chan, Y. Wang, C.-M. Che, K.-K. Cheung, N. Zhu, *Chem. Eur. J.* **2001**, *7*, 4180 and references cited therein. [13b] J. Brook, Y. Babayan, S. Lamansky, P. I. Djurovich, I. Tsyba, R. Bau, M. E. Thompson, *Inorg. Chem.* **2002**, *41*, 3055.

[14] The emission spectra of all complexes, except **2**, in the solid state exhibit red-shifted and broader bands with similar maximum emission wavelengths to those of the corresponding spectra in solution under the same conditions. In contrast, complex **2** still shows a blue-shifted emission in the solid state relative to [Ir(ppy)$_3$].

[15] J. R. Lakowicz, *Principles of Fluorescence Spectroscopy*, Kluwer Academic, New York, **1999**.

[16] L. S. Sapochak, A. Padmaperuma, N. Washton, F. Endrino, G. T. Schmett, J. Marshall, D. Fogarty, P. E. Burrows, S. R. Forrest, *J. Am. Chem. Soc.* **2001**, *123*, 6300.

[17] [17a] P. A. Lane, L. C. Palilis, D. F. O'Brien, C. Giebeler, A. J. Cadby, D. G. Lidzey, A. J. Campbell, W. Blau, D. D. C. Bradley, *Phys. Rev. B.* **2001**, *63*, 235206. [17b] D. F. O'Brien, C. Giebeler, R. B. Fletcher, A. J. Cadby, L. C. Palilis, D. G. Lidzey, P. A. Lane, D. D. C. Bradley, W. Blau, *Synth. Met.* **2001**, *116*, 379. [17c] X. Gong, J. C. Ostrowski, D. Moses, G. C. Bazan, A. J. Heeger, *Adv. Funct. Mater.* **2003**, *13*, 439.

[18] The emission bands originating from CBP (host) or NPD at a lower concentration (0.1 wt.-%) of dopant (Ir complexes) in EL devices were not observed in all cases.

[19] *SHELXTL NT Crystal Structure Analysis Package*, version 5.14, Bruker AXS, Analytical X-ray System, Madison, WI, USA, **1999**.

[20] K.-M. Park, I. Yoon, B. S. Yoo, J. B. Choi, S. S. Lee, B. G. Kim, *Acta Crystallogr., Sect. C* **2000**, *56*, 1191.

Received February 12, 2004
Early View Article
Published Online June 15, 2004

